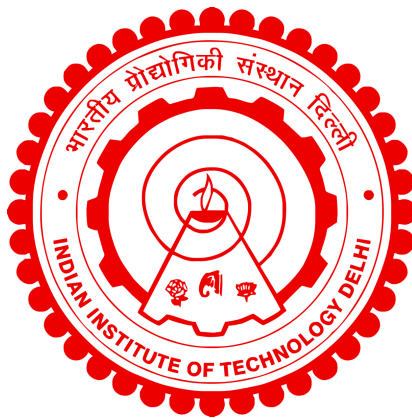


**TOTAL INTERNAL REFLECTION  
FLUORESCENCE AND SCATTERING  
IMAGING FOR BIOLOGICAL APPLICATIONS**

**ARTI TYAGI**



**DEPARTMENT OF BIOCHEMICAL ENGINEERING  
AND BIOTECHNOLOGY**

**INDIAN INSTITUTE OF TECHNOLOGY DELHI**

**FEBRUARY 2023**



© Indian Institute of technology Delhi (IITD), New Delhi, 2023



**TOTAL INTERNAL REFLECTION  
FLUORESCENCE AND SCATTERING  
IMAGING FOR BIOLOGICAL APPLICATIONS**

by

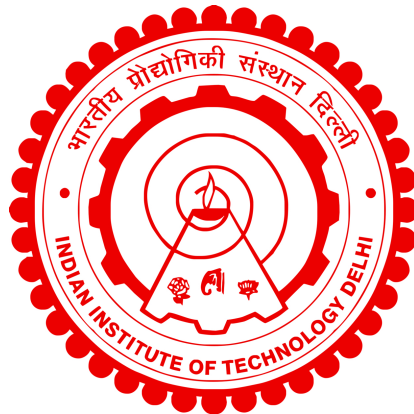
**ARTI TYAGI**

Department of Biochemical Engineering and Biotechnology

Submitted

in partial fulfillment of the requirements of the degree of Doctor of Philosophy

to the



**INDIAN INSTITUTE OF TECHNOLOGY  
DELHI**

**FEBRUARY 2023**



*Dedicated to Amma, Maa and Papa*



---

# Certificate

This is to certify that the thesis entitled '**Total internal reflection fluorescence and scattering imaging for biological applications**', submitted by **Arti Tyagi** to the Indian Institute of Technology Delhi, for the award of the degree of **Doctor of Philosophy** in February 2023, is a record of the original, bonafide research work carried out by her under my supervision and guidance. The thesis has reached the standards fulfilling the requirements of the regulations related to the award of the degree.

The results contained in this thesis have not been submitted in part or in full to any other University or Institute for the award of any degree or diploma to the best of my knowledge.

**Prof. Ravikrishnan Elangovan**

Department of Biochemical Engineering and Biotechnology,  
Indian Institute of Technology Delhi



# *Acknowledgements*

PhD has been a very challenging phase of my life, academically, physically, mentally and emotionally. It would not have been possible to achieve this monumental feat without crucial support from a lot of people. The last five and a half years have taught me so many things and shaped me into someone with a never-ending curiosity and zeal to understand and learn.

The list of people I would like to thank could be very long. I will begin by expressing my deepest gratitude to my parents, Mr. Khushpal Singh and Mrs. Neelam Tyagi, for always standing by me in all my decisions, for having faith in me, and encouraging me to keep on doing better. Next, I would like to thank the one person who has been the biggest driving force behind this journey, my supervisor, Prof. Ravikrishnan Elangovan. I remember how naive and inexperienced I was when I entered his laboratory. He has been extremely patient and thoughtful with me. I will forever be thankful to him for introducing me to applied optics, a field I have come to love and enjoy. Other than research aptitude and acumen, I have learnt important skills of time management, delegation, planning, execution and documentation from him, which will help me wherever I go.

My SRC members, Prof. Kedar Khare, Prof. Ritu Kulshreshtha and Prof. Ashish Misra, have also been very forthcoming with constructive criticism as well as encouragement and appreciation. The discussions I have had with Prof. Khare have been extremely informative and helpful for my work. I was also involved in a collaborative project with AIIMS and through that I received critical support from members of the Oncology department at AIIMS, Dr. Sachin Singla, Dr. Prabhat Singh Mallik and Dr. Amit Dinda. Without their contributions, it would have been nearly impossible to carry out the SNC-TIRS work. Similarly, I received a great deal of help from an inter-disciplinary team of exceptional engineers from one of our lab projects. Mr. Pabhu Balsubramanian, Mr. Bramha Tripathi, and Mr. Tushar Jeet brought along their individual expertise and helped me develop the *i-scope* system.

Other than my professors and colleagues, several of my labmates and friends have been instrumental in completion of my thesis. During my initial years, I acquired a lot of hands-on-experience and instrument knowledge from my seniors, Dr. Pooja

Singh, Dr. Saumya Singh, Dr. Vidhu Soman, and Ms. Jyoti Sharma. These people helped me understand how to effectively function inside a laboratory atmosphere and inculcated a healthy working environment. I have received considerable support and help from the members of our neighbouring laboratory of Prof. Prashant Mishra. His students, Dr. Sanjay Singh and Dr. Senthil Murugan were always ready to share their knowledge as well as laboratory resources with us. I have also been fortunate enough to have amazing labmates and friends, Ms. Shefali Singh, Ms. Neha Khaware, Mr. Jagat Narayan, Ms. Sneha Kumari, Ms. Neelam Upadhyay, and Ms. Ada Zwetlana. They have all taught me so many new things in such varied disciplines, helped me carry out experiments, and always been there for me when I needed them for both work as well as fun!

Other than the academic influences and support, I have been the subject of tremendous moral support and aid from my brother, Mr. Dharmanshu Tyagi and long time friends, Ms. Shalini Goyal, Mr. Shubham Gupta, Ms. Vismaya Vinay, Mr. Himanshu Pandey, and Mr. Ashish Gopalakrishnan. It is very well known that a PhD can be an emotionally taxing time, and without these people it would not have been possible to go through all the ups and downs I have faced throughout this journey.

At last, I would express my sincere thanks to the Indian Institute of Technology Delhi and especially to the Department of Biochemical Engineering and Biotechnology for choosing me to be part of the IITD family and providing me with the means and opportunities to carry out this work. I would also thank the Ministry of Human Resource and Development, Government of India for providing me with financial support through the five years of my PhD.

## सारांश

जैविक इमेजिंग एक अत्यंत उपयोगी और लोकप्रिय विश्लेषणात्मक उपकरण है। इसने सूक्ष्मदर्शी तकनीकों में होती प्रगति से महत्वपूर्ण लाभ उठाया है और गुणात्मक के साथ-साथ मात्रात्मक जानकारी प्राप्त करने के एक विश्वसनीय स्रोत के रूप में उभरा है। जैविक इमेजिंग में कंट्रास्ट उत्पन्न करने के दो व्यापक साधन प्रतिदीप्ति (फ्लूरोसेंस) और प्रकाश प्रकीर्णन (स्कैटरिंग) हैं। ये अलग-अलग तरीके हैं जिनसे प्रकाश, एक विद्युत चुम्बकीय विकिरण, पदार्थ के साथ संपर्क करता है। प्रतिदीप्ति में इलेक्ट्रॉनिक राज्य संक्रमणों के परिणामस्वरूप चयनात्मक तरंगदैर्घ्य का अवशोषण और उत्सर्जन शामिल है। दूसरी ओर, प्रकीर्णन ज्यादातर कंपन संक्रमणों के परिणामस्वरूप होता है, जिसमें एक नमूने पर पड़ने वाली प्रकाश किरणें अलग-अलग दिशाओं में विक्षेपित होती हैं। इमेजिंग विधियों और अनुप्रयोगों के संबंध में दोनों तकनीकों अद्वितीय लाभ और हानि की पेशकश करती हैं। अनुसंधान और वाणिज्यिक उद्देश्यों के लिए उपलब्ध मौजूदा इमेजिंग सिस्टम द्वारा प्रदान किए जाने वाले विभिन्न लाभों के बावजूद, इनमें से अधिकांश मामलों में एक सामान्य सीमित कारक है उपकरण और रखरखाव की उच्च लागत। ये प्रणालियां अक्सर भारी उपकरणों पर आधारित होती हैं और प्रशिक्षित ऑपरेटरों की आवश्यकता रखती हैं। इसलिए, आज हमें कॉम्पैक्ट, लागत-प्रभावी, तेज़ और उपयोग में आसान इमेजिंग आधारित प्लेटफॉर्म की आवश्यकता है।

इस काम में मैंने कुल आंतरिक प्रतिबिंब-आधारित ऑप्टिकल मॉड्यूल को नियोजित करके व्यापक संभावित जैविक अनुप्रयोगों के साथ दो इमेजिंग सिस्टम विकसित किए हैं। पहले मामले में, एक पूरी तरह से स्वचालित और लघु सूक्ष्मदर्शी प्रणाली, जिसे आइ-स्कोप कहा जाता है, विकसित किया गया है। यह उच्च आवर्धन एवं संकल्प, बड़े क्षेत्र के दृश्य और बड़े क्षेत्र नमूना स्कैनिंग जैसी सुविधाएं प्रदान करता है। सिस्टम में अधिकांश उद्घृत या स्वविकसित थ्रीडी-प्रिंटेड घटकों के साथ एक सरलीकृत डिज़ाइन शामिल है। यह एक ब्राइटफ़्रील्ड और (कुल आंतरिक प्रतिबिंब) प्रतिदीप्ति मोड में नमूना इमेजिंग की सुविधा देता है। आइ-स्कोप का उपयोग दूध दैहिक कोशिकाओं और जीवाणुओं की कोशिका गणना के लिए किया गया है। यह पारंपरिक प्रतिदीप्ति सूक्ष्मदर्शी (फ्लोरोसेंस माइक्रोस्कोप) के स्थान पर एक लागत-प्रभावी, पोर्टेबल, स्वचालित और सुविधाजनक विकल्प प्रदान करता है।

दूसरे मामले में, एसएनसी-टीआईआरएस नामक एकल कण ट्रैकिंग पर आधारित एक लेबल-मुक्त नैनोपार्टिकल लक्षण वर्णन प्रणाली विकसित की गई है। सिस्टम एक इवनेसेंट फ़्रील्ड (लुप्त होने वाली) के साथ नमूना कणों को रोशन करता है और कण प्रक्षेपवक्र को मैप करने के लिए बिखरे हुए प्रकाश को इकट्ठा करता है। कणों के हाइड्रोडायनामिक आकार का अनुमान लगाने के लिए एकल कण प्रक्षेपवक्र का उपयोग किया जाता है। इसके अलावा, नमूने में कणों की कुल मात्रा का अनुमान लगाने के लिए अवलोकन मात्रा निर्धारित की जाती है। एसएनसी-टीआईआरएस का मूल्यांकन अकार्बनिक नैनोकणों के साथ-साथ एक्सोसोम नामक जैविक नैनो-पुटिकाओं का उपयोग करके किया गया है।

इस थीसिस कार्य की एक एकीकृत विशेषता उन विधियों और प्रणालियों को विकसित करना है जो, विशेष रूप से सीमित-संसाधन क्षेत्रों में, अधिक सुलभ हैं। आइ-स्कोप और एसएनसी-टीआईआरएस दोनों की अवधारणा और विकास प्रक्रियाएं इस दृष्टिकोण से प्रेरित थीं। दोनों प्रणालियां कोई विस्तृत ढांचागत या नमूना पूर्व-उपचार आवश्यकताओं से बाध्य नहीं हैं। इसके अलावा, वे उपयोगी नैदानिक उपकरण के रूप में काम करने की क्षमता प्रदर्शित करते हैं।

# *Abstract*

Biological imaging is an immensely useful and popular analytical tool. It has gained significantly with advances in microscopic techniques and has emerged as a reliable source of qualitative as well as quantitative information. Two of the most widely used means of contrast generation for biological imaging are fluorescence and light scattering. These are different ways in which light, an electromagnetic radiation, interacts with matter. Fluorescence involves absorption and emission of selective wavelengths as a result of electronic state transitions. Scattering, on the other hand, is more of a result of vibrational transitions wherein light incident on a sample is deflected in different directions. Both techniques offer unique pros and cons with regards to imaging methods and applications. Notwithstanding the various advantages offered by the existing imaging systems available for research and commercial purposes, a common limiting factor in most of these cases is the high cost of instrumentation and maintenance. These systems are also often bulky and require trained operators, and hence, there is a need for compact, cost-effective, rapid and easy-to-use imaging based platforms.

In this work I have developed two imaging systems with wide potential biological applications by employing a total internal reflection-based optical module. In the first case, a fully automated and miniaturized microscopy system, called the *i-scope*, has been developed which offers features such as a high magnification, resolution, larger field-of-view and a large-area sample scanning. The system comprises of a simplistic design with off-the-shelf or in-house 3D printed components. It allows sample imaging in a brightfield and (total internal reflection) fluorescence modes. The *i-scope* has been used for cell enumeration of milk somatic cells and bacteria. It offers a cost-effective, portable, automated and convenient alternative to conventional fluorescence microscopes.

In the second case, a label-free nanoparticle characterisation system based on single particle tracking, called SNC-TIRS, is developed. The system illuminates sample particles with a evanescent field and collects the scattered light to map particle trajectories as they diffuse through the observation volume. The single particle trajectories are used to estimate hydrodynamic sizes of the particles. Moreover, the observation volume is quantified to estimate sample concentration. SNC-TIRS

has been evaluated using inorganic nanoparticles as well as biological nano-vesicles called exosomes.

A unifying feature of this thesis work has been to develop methods and systems which are more accessible, especially in low-resource field settings. The conceptualisation and development processes of both *i-scope* and SNC-TIRS were driven by this approach. Both systems do not impose any elaborate infrastructural or sample pre-treatment requirements. Furthermore, they display potential to serve as useful diagnostic tools.

# Contents

Certificate

Acknowledgements

Abstract

Contents

List of Figures

List of Tables

<b>1</b>	<b>Introduction</b>	<b>1</b>
1.1	Thesis Objectives . . . . .	3
1.2	Thesis Organisation . . . . .	4
<b>2</b>	<b>Theory and Literature Review</b>	<b>5</b>
2.1	Fluorescence Imaging Systems . . . . .	5
2.1.1	Fluorescence . . . . .	5
2.1.2	Fluorescence Microscopy . . . . .	7
2.1.2.1	Fluorophores and filters . . . . .	8
2.1.2.2	Epi-fluorescence, filter cubes, and detectors . . . . .	8
2.1.2.3	Objective lenses . . . . .	11
2.1.2.4	Light sources . . . . .	12
2.1.3	Miniaturization of Fluorescence Microscopy . . . . .	13
2.1.4	Automation of Fluorescence Imaging and Analysis . . . . .	17
2.2	Scattering Imaging Systems . . . . .	19
2.2.1	Light scattering: Theory and Types . . . . .	19
2.2.2	Biological Imaging with Scattered Light . . . . .	22
2.3	Total Internal Reflection . . . . .	25

2.3.1	TIR: Theory and Historical Perspectives . . . . .	25
2.3.2	cTIRF: A compact TIR module . . . . .	32
2.4	Applications . . . . .	32
2.4.1	Cell count based diagnostics . . . . .	33
2.4.2	Nanoparticle characterization . . . . .	34
<b>3</b>	<b><i>i-scope</i>: Miniaturized fluorescence microscopy system for point-of-care applications</b>	<b>38</b>
3.1	Materials and Methods . . . . .	39
3.1.1	Optical and Mechanical Components . . . . .	39
3.1.2	Chemical Reagents . . . . .	40
3.1.3	Biological Samples . . . . .	40
3.1.4	The <i>i-scope</i> Concept and Design . . . . .	40
3.1.4.1	<i>i-scope</i> v1.1 Optical Assembly . . . . .	45
3.1.4.2	<i>i-scope</i> v1.1 Mechanical Assembly . . . . .	47
3.1.4.3	<i>i-scope</i> v1.1 Electronic Assembly . . . . .	50
3.1.4.4	<i>i-scope</i> v1.2 . . . . .	50
3.1.4.5	<i>i-scope</i> Data Acquisition and Analysis Program . . . . .	51
3.1.4.6	Sample Preparation for Microscopy . . . . .	53
3.2	Results . . . . .	54
3.3	Discussion . . . . .	55
<b>4</b>	<b>Cell count based diagnostics</b>	<b>59</b>
4.1	Materials and Methods . . . . .	59
4.1.1	Chemical Reagents . . . . .	59
4.1.2	Biological Samples . . . . .	60
4.1.3	Somatic Cell Isolation . . . . .	60
4.1.4	<i>Mycobacterium smegmatis</i> Culture . . . . .	61
4.1.5	Sample Preparation for Microscopy . . . . .	61
4.1.6	Data Acquisition and Analysis with <i>i-scope</i> . . . . .	62
4.1.7	Data Acquisition and Analysis with Microscope . . . . .	63
4.2	Results . . . . .	64
4.2.1	Tests with Somatic Cells . . . . .	64
4.2.2	Tests with <i>M. smegmatis</i> . . . . .	66
4.3	Discussion . . . . .	68
<b>5</b>	<b>SNC-TIRS: A label-free nanoparticle characterization system</b>	<b>73</b>
5.1	Materials and Methods . . . . .	76
5.1.1	Chemical reagents and other materials . . . . .	76
5.1.2	Biological Samples . . . . .	76
5.1.3	Nanoparticle Sample preparation . . . . .	77

5.1.4	Preparation of Magnetic Nanoparticle-Antibody (MNP-Ab) Conjugates . . . . .	77
5.1.5	Exosome Isolation and Sample Preparation . . . . .	78
5.1.5.1	Exosome Isolation using Immunomagnetic Capture . . . . .	78
5.1.5.2	Exosome Isolation using Precipitation . . . . .	78
5.1.6	Dynamic Light Scattering (DLS) . . . . .	79
5.1.7	High Resolution Transmission Electron Microscopy (HR-TEM) . . . . .	79
5.1.8	Nanoparticle Tracking Analysis (NTA) . . . . .	80
5.1.9	Data Acquisition with SNC-TIRS system . . . . .	80
5.1.10	Data Analysis with SNC-TIRS system . . . . .	81
5.2	Results . . . . .	82
5.2.1	Size Estimation of MNPs and GNPs . . . . .	82
5.2.2	Particle Sub-population Analysis for MNPs . . . . .	82
5.2.3	Concentration Estimation of MNPs . . . . .	83
5.2.4	Size Estimation of MNP-Ab conjugates and exosomes . . . . .	85
5.3	Discussion . . . . .	90
5.3.1	Size estimation and sub-population analysis of nanoparticles . . . . .	91
5.3.2	Effects of Surface Proximity on Size Estimation . . . . .	92
5.3.3	Concentration estimation of nanoparticles . . . . .	94
5.3.4	Analysing exosomes with SNC-TIRS . . . . .	95
5.3.5	SNC-TIRS compared to NTA and DLS . . . . .	96
<b>6</b>	<b>Summary and Future Prospects</b>	<b>99</b>
6.1	<i>i-scope</i> : Development, performance optimisation, and application . . . . .	100
6.2	SNC-TIRS: Development, performance optimisation, and application . . . . .	102
<b>7</b>	<b>References</b>	<b>105</b>
<b>8</b>	<b>List of Publications</b>	<b>121</b>
<b>9</b>	<b>Author Biodata</b>	<b>122</b>

# List of Figures

2.1	A Jablonski diagram depicting the various electronic state transitions leading to fluorescence and phosphorescence . . . . .	7
2.2	Optical schematic of a standard epi-fluorescence microscope. White light from a light source filters through optical filters and dichroic mirror to specifically illuminate the sample via an objective lens. Subsequently, a higher wavelength of emitted light is collected via the same objective lens and imaged with a detector. . . . .	10
2.3	Optical schematic of (A) A finite-tube length microscope, and (B) An infinity-corrected microscope. The infinity-corrected optics contains an additional tube lens which creates a parallel light path between the objective lens and the tube lens to introduce any additional optical components. . . . .	13
2.4	A Jablonski diagram depicting the virtual state transitions involved in different types of light scattering . . . . .	20
2.5	Directional dependence of Rayleigh and Mie scattering . . . . .	22
2.6	Optical schematic of a dark field microscope. Light from the source is passed through a dark field condenser which allows selective transmission of light such that the illuminating light rays do not reach the objective lens. Only light scattered by the sample is, thus, collected by the objective which results in better imaging contrast. . . . .	24
2.7	Schematic representation of interferometric scattering microscopy using (A) the primary light source to illuminate the sample as well as the reference beam for interference; and (B) two different light sources for sample illumination and as reference beam. . . . .	26
2.8	Behaviour of light rays as they travel from a denser to a rarer medium, depending on the angle of incidence ( $\theta_i$ ). Total internal reflection occurs when $\theta_i$ exceeds a critical angle ( $\theta_c$ ). The inset in C depicts behaviour of an evanescent field generated as a result of this, whose intensity decays exponentially on moving away from the interface of the two media . . . . .	28
2.9	The two major types of TIR schemes. (A) A prism is optically coupled to the coverslip surface placed on top of the sample. Light refracted by the prism undergoes TIR. (B) A high NA objective lens is used to generate TIR by sending light rays only through the lens' periphery. . . . .	30

2.10	(A) An optical waveguide depicting the core and cladding layers giving rise to multiple total internal reflections. (B) Optical waveguide-based microscopy. . . . .	31
2.11	A schematic diagram of the original cTIRF module showing all its optical components. Pandey, V. <i>et al</i> , 2018 . . . . .	32
3.1	Schematic representation of the initial idea of <i>i-scope</i> using a single lens for magnification and a USB camera for imaging . . . . .	41
3.2	The first iteration of the <i>i-scope</i> device which contained only a biconvex lens and a USB camera. It was made out of an acrylic sheet and used ambient light for sample illumination. . . . .	41
3.3	The journey of <i>i-scope</i> with many design, component, and operational changes over some iterations. . . . .	44
3.4	The final iteration of <i>i-scope</i> v1.1, with its top lid opened and a monitor, keyboard and mouse attached. The monitor displays Page one of the <i>i-scope</i> program . . . . .	45
3.5	A schematic representation of the optical assembly of <i>i-scope</i> . . . . .	48
3.6	A 3D model of the <i>i-scope</i> assembly showing the various mechanical (and optical) components. The external casing is not shown here. . . . .	49
3.7	A block diagram of <i>i-scope</i> assembly showing the various electronic components . . . . .	51
3.8	GUI of the <i>i-scope</i> data acquisition and analysis program, showing (A) Page one and (B) Page two, with the various functions . . . . .	52
3.9	A stage micrometer imaged using (A) <i>i-scope</i> v1.1 and (B) <i>i-scope</i> v1.2 . . . . .	55
3.10	1 $\mu$ m sized Fluorescent polystyrene beads imaged using (A) <i>i-scope</i> v1.1 and (B) <i>i-scope</i> v1.2 . . . . .	56
3.11	HL60 cells imaged using a conventional inverted fluorescence microscope with a 50X air-objective lens under (A) brightfield mode, and (B)fluorescence mode. The same sample was imaged using <i>i-scope</i> v1.1 under (C)brightfield mode, (D)fluorescence mode. and <i>i-scope</i> v1.2 under (E)brightfield mode, (F)fluorescence mode. Cells were labelled with acridine orange for fluorescence imaging and with methylene blue for brightfield imaging with <i>i-scope</i> v1.2. . . . .	57
4.1	Different steps of the process of somatic cell isolation and enumeration. . . . .	60
4.2	Somatic cells isolated from raw cow milk and spiked in 1X PBS observed under the brightfield mode with (A) Microscope; B) <i>i-scope</i> ; and under the fluorescence mode with (C) Microscope; (D) <i>i-scope</i> . . . . .	65
4.3	Somatic cells isolated from raw cow milk, spiked in 1X PBS, labelled with (A) CFSE, and (B) Acridine orange as observed under the fluorescence mode with <i>i-scope</i> . . . . .	65
4.4	Somatic cells spiked in milk diluted with 1X PBS in a 1:1 ratio, observed under (A) Microscope and (B) <i>i-scope</i> . . . . .	66

4.5	Average number of somatic cells observed per frame as a function of the sample concentration, using (A) Microscope, and (B) <i>i-scope</i> . Four additional dilutions have been shown in the inset of (B). The error bars display the standard deviation in triplicates. . . . .	66
4.6	<i>M. smegmatis</i> observed under the brightfield mode with (A) Microscope; (B) <i>i-scope</i> ; and under the fluorescence mode with (C) Microscope; (D) <i>i-scope</i> . . . . .	67
4.7	Average number of <i>M. smegmatis</i> observed per frame as a function of the sample concentration, using (A) Microscope, and (B) <i>i-scope</i> . The error bars display the standard deviation in triplicates. . . . .	68
5.1	(A) A schematic representation of the SNC-TIRS setup. The cTIRF module is used to illuminate nanoparticles diffusing in an aqueous suspension using an evanescent field (inset). Light scattered by the particles is collected by a 50X air-objective. (B) A photograph of the cTIRF module with its laser switched on showing the waveguide pattern formed throughout the glass slide due to repeated TIR. (C) 100nm-sized MNPs (MNP Sample I) imaged using the SNC-TIRS system. The scale bar represents 5 $\mu$ m. (D) Single particle trajectories plotted for the MNPs imaged in (C). (E) A plot of MSD against lag time for the trajectories obtained in (D). . . . .	75
5.2	Hydrodynamic sizes of inorganic nanoparticle samples estimated by DLS and SNC-TIRS for: GNPs (Manufacturer reported size 80 nm), MNP I (Manufacturer reported size 100 nm), MNP II (Manufacturer reported size 130 nm), MNP III (Manufacturer reported size 230 nm), and MNP IV (Manufacturer reported size 250 nm). The linear fit has an R <sup>2</sup> (adjusted) value = 0.993. Error bars denote standard deviation. . . . .	83
5.3	Size of MNP Sample I measured by SNC-TIRS at 27°C and 33°C. Size distribution histograms at both temperatures are displayed with a Gaussian fit. Average size and standard deviation are reported in each case. . . . .	84
5.4	Single-particle size analysis of MNP samples I to IV showing population distributions estimated by SNC-TIRS. Each histogram reflects data collected from 100 particles. A Gaussian fit is applied and the mean sizes along with the standard deviation values are shown. . . . .	85
5.5	A) Mean particle number observed in a movie with SNC-TIRS as a function of manufacturer reported (known) concentration values. A linear fit has been applied with an $R^2$ (adjusted) value of 0.983. B) MNP concentrations estimated by SNC-TIRS as a function of manufacturer reported (known) concentrations. A linear fit has been applied with an $R^2$ (adjusted) value of 0.950. Error bars in both plots represent standard deviation. . . . .	86

5.6	Particle size distributions of MNPs, MNP-Antibody, MNP-Antibody-Exosome immunomagnetically isolated from a plasma sample, and exosomes isolated via precipitation method. Each distribution plot is based on data from 60 individual particles/conjugates. . . . .	87
5.7	A) Detection of exosomes isolated from plasma sample using size estimation by SNC-TIRS. Data shown here is an average of 60 individual particles for each of the four samples: exosomes isolated via precipitation method, MNPs, MNP-Antibody and MNP-Antibody-Exosome isolated from a single plasma sample. The data labels indicate the average values while the error bars depict standard deviation. B) High-resolution TEM (HR-TEM) image of MNP-Antibody-Exosome with a scale bar of 200 nm at the bottom. The darker irregularly shaped MNPs can be seen separated from the lighter spherical exosomes. C) HR-TEM image of only exosomes isolated via the precipitation method with a scale bar of 200 nm at the bottom. . . . .	88
5.8	Sizes estimated for all the clinical isolated by (A) DLS versus SNC-TIRS, and (B) NTA versus SNC-TIRS. The linear curve fit has an $R^2$ value (adj.) of 0.87 and 0.83 respectively, and the error bars denote standard deviation. (C) Distribution of sizes obtained estimated by SNC-TIRS and NTA for a sample of MNP-Ab-exosomes. . . . .	89
5.9	Distribution of particle-surface separation (h) with respect to SNC-TIRS estimated particle sizes for (A) 230nm and (B) 250nm sized MNPs. Distribution of particle scattering intensities with respect to SNC-TIRS estimated particle sizes for (C) 230nm and (D) 250nm sized MNPs . . . . .	94

# List of Tables

3.1	Cost analysis of the complete <i>i-scope</i> system. . . . .	43
4.1	A comparison of the performances of some contemporary systems with <i>i-scope</i> . . . . .	72
5.1	A comparison of performances of the three nanoparticle characteriza- tion methods: DLS, NTA and SNC-TIRS . . . . .	98

## *Abbreviations*

---

**App** Application

**3D** Three Dimensional

**TIRF** Total Internal Reflection Fluorescence

**TIRFM** Total Internal Reflection Fluorescence Microscopy

**cTIRF** Compact Total Internal Reflection Fluorescence

**TIRS** Total Internal Reflection Scattering

**GUI** Graphical User Interface

**LED** Light Emitting Diode

**MJP** MultiJet Printer

**NA** Numerical Aperture

**SNR** Signal-to-noise Ratio

**Webcam** Web camera

**f/#** F-number

**v/v** Volume-by-volume ratio

**DMSO** Dimethyl Sulfoxide

**TB** Tuberculosis

**AFB** Acid Fast Bacillus

**NSCLC** Non-Small Cell Lung Cancer

**PCB** Printed Circuit Board

**TEM** Transmission Electron Microscopy

**HR-TEM** High Resolution-Transmission Electron Microscopy

**R.I.** Refractive Index

**RBC** Red Blood Cell

**WBC** White Blood Cell

**FOV** Field-of-view